

Host isotope effect on the localized vibrational modes of oxygen in isotopically enriched ^{28}Si , ^{29}Si , and ^{30}Si single crystals

Jiro Kato and Kohei M. Itoh

*Department of Applied Physics and Physico-Informatics, Keio University, Yokohama 223-8522, Japan
and CREST-JST, Japan*

Hiroshi Yamada-Kaneta

Nano-electronic Materials Laboratory, Fujitsu Laboratories Limited, 10-1 Morinosato-Wakamiya, Atsugi 243-0197, Japan

Hans-Joachim Pohl

Vitcon Projectconsult GmbH, Dornbluthweg 5, D-07743, Jena, Germany

(Received 27 March 2003; published 10 July 2003)

A high-resolution infrared absorption study of the localized vibrational modes (LVM's) of oxygen in isotopically enriched ^{28}Si , ^{29}Si , and ^{30}Si single crystals is reported. Isotope shifts of LVM frequencies from those in natural Si are clearly observed not only due to the change of the average mass in the nearest-neighbor silicon atoms, but also to the combined effect of the (i) change in Si masses of the second and beyond nearest neighbors and (ii) change in the lattice constants of the host Si crystals. These conclusions have been drawn based on a direct comparison between the experimental results and theoretical calculations assuming harmonic potentials for localized vibrations of oxygen. However, the LVM linewidths of the A_{2u} mode in the enriched samples are much narrower than those in natural Si, despite the fact that the harmonic approximation predicts very little dependence of the width on the host Si isotopic composition. This observation suggests that both anharmonicity and inhomogeneous broadening due to isotopic disorder are playing important roles in the determination of oxygen LVM linewidths. Moreover, a new series of oxygen LVM peaks is observed clearly in the isotopically enriched samples thanks to the small degree of mass disorder.

DOI: 10.1103/PhysRevB.68.035205

PACS number(s): 63.20.Pw, 78.30.Am

I. INTRODUCTION

A wide variety of novel isotope effects have been discovered recently,¹⁻⁵ thanks to the availability of high-quality bulk Si crystals with controlled isotopic compositions.^{6,7} In contrast to well-behaved isotope effects on phonons in Si crystals with relatively mixed isotopic compositions,² unpredictable isotope effects have been discovered more recently in nearly 100% monoisotopic Si crystals.³⁻⁵ With respect to the results obtained with natural silicon (hereafter $^{\text{nat}}\text{Si}$), which has the isotopic composition ^{28}Si (92.23%), ^{29}Si (4.67%), and ^{30}Si (3.10%), a dramatic increase in thermal conductivity,³ a significant narrowing of the impurity bound exciton luminescence peaks,⁴ and absence of acceptor ground-state splitting⁵ have been found unexpectedly when the enrichment of ^{28}Si exceeded 99.98%. Similarly, a surprisingly large isotope effect on hydrogenic impurity levels has been reported for isotopically enriched diamond.⁸ The present paper reports another intriguing isotope effect on the localized vibrational mode (LVM) of oxygen in silicon.

Because of its technological importance, the behavior of oxygen in silicon has been studied extensively.⁹ As a result, rich physics associated with the localized motion of light impurities embedded in a relatively heavy host matrix¹⁰ has been revealed using oxygen in silicon as one of the ideal examples. An oxygen atom in silicon tends to exist as an interstitial defect between two silicon atoms in the $\langle 111 \rangle$ direction as shown in Fig. 1.¹¹⁻¹⁵ *Ab initio* calculations have shown the bond lengths of Si-O to be 1.59 Å, with the most

probable Si-O-Si bond angle 172° .¹⁶ An interstitial oxygen atom has 2 equivalent nearest-neighbor Si atoms, 6 equivalent second-nearest-neighbor Si atoms, 18 equivalent third-neighbor Si atoms, and so on. In the framework of the harmonic approximation, frequencies of LVM's of oxygen in silicon are determined by the local structures and masses (i.e., isotopes) of vibrating oxygen and neighboring Si atoms. In many cases the isotope shifts of the spring constants k and K of Si-O and Si-Si bonds, respectively, are small enough to be ignored. Therefore, isotope substitution of the oxygen centers with ^{16}O , ^{17}O , and ^{18}O , which changes exclusively the mass of vibrating species, has been useful in the past for experimental understanding of the LVM of oxygen in silicon. Moreover, the discovery that the LVM linewidth of ^{17}O is a factor of 1.5 larger than those of ^{16}O and ^{18}O in $^{\text{nat}}\text{Si}$ has suggested strongly that the interaction between Si phonons and oxygen LVM's determines the lifetime of the oxygen LVM's in silicon.¹⁴

In order to understand the interaction between the bulk Si isotopes and vibrating oxygen atoms, two factors must be considered separately: (i) the energy dependence of the multiphonon emissivity, which is determined mainly by the average mass of the constituent Si isotopes, and (ii) disorder in Si masses (disorder in the Si isotope distribution), which arises from the copresence of ^{28}Si , ^{29}Si , and ^{30}Si isotopes. While the larger linewidth of ^{17}O is most likely due to the former effect, the effect of isotopic disorder is predicted to be negligibly small within the framework of the harmonic approximation, as we will show later. As a result, the LVM linewidth is believed to be determined solely by the relation between the LVM frequency (which depends on the masses

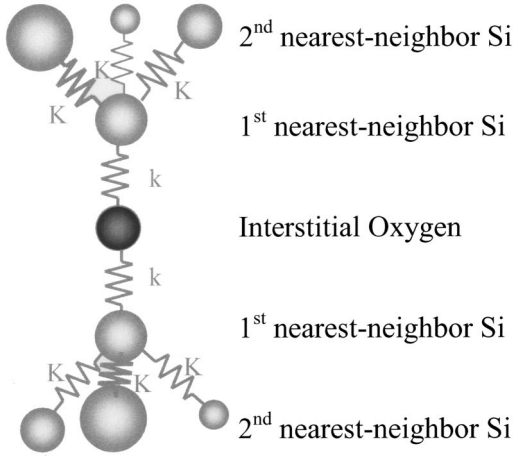


FIG. 1. Interstitial oxygen atom in a Si crystal.

of the oxygen and neighboring Si atom) and the emissivity of Si phonons. However, recent pump and probe measurements of the oxygen LVM in ^{nat}Si revealed an LVM lifetime of 229 ps, which translates to a width of 0.023 cm^{-1} (Ref. 17); i.e., the linewidths measured in the absorption measurement are likely to be inhomogeneously broadened.

The present paper reports on the surprisingly large effect of Si isotopic mass disorder on oxygen LVM's, which cannot be explained very well by the harmonic approximation, but clearly is one of the main origins for the line broadening observed previously.

II. EXPERIMENTAL PROCEDURES

Similar to the recent experiments on oxygen LVM's in isotopically controlled Ge,^{18,19} the present work has investigated LVM's of oxygen in Si samples with controlled isotopic composition. Isotopic composition and oxygen concentration [O] of four samples investigated are listed in Table I. The Si isotopic composition and oxygen concentration of each sample were determined using secondary-ion mass spectrometry (SIMS) and IR absorption based on the American Standard for Testing and Materials F121-79, respectively. The electrically active net-impurity concentration of each sample as determined by the Hall effect is less than 10^{16} cm^{-3} , and the carbon concentration is much less than the order of 10^{17} cm^{-3} since the absorption due to carbon LVM's in Si (measured at 607 cm^{-1} for ^{nat}Si) was not observed. Oxygen LVM spectra have been recorded with a BOMEM DA-8 Fourier transform spectrometer equipped with a Globar light source, a KBr beam splitter, and a

TABLE I. Isotopic composition and oxygen concentration of the measured samples.

| Sample | ^{28}Si [%] | ^{29}Si [%] | ^{30}Si [%] | Oxygen [cm^{-3}] |
|--------|----------------------|----------------------|----------------------|-----------------------------|
| SI-28 | 99.86 | 0.13 | 0.01 | 4.75×10^{17} |
| SI-29 | 2.17 | 97.10 | 0.73 | 1.01×10^{18} |
| SI-30 | 0.67 | 0.59 | 98.74 | 8.79×10^{17} |
| SI-nat | 92.2 | 4.7 | 3.1 | 6.49×10^{17} |

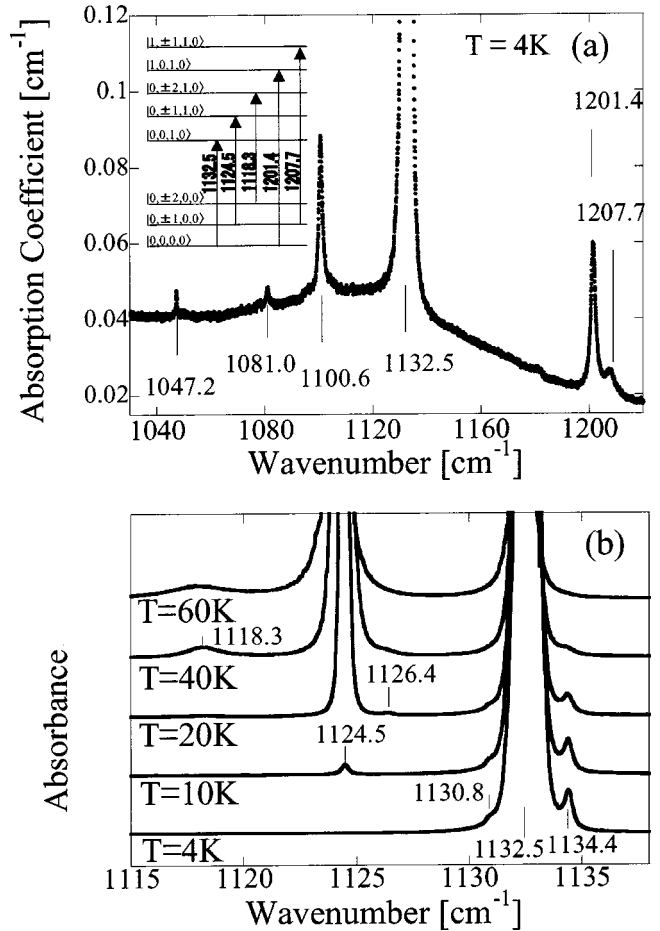


FIG. 2. (a) Absorption spectrum of the SI-29 sample measured at $T = 4 \text{ K}$ and (b) temperature dependence of the A_{2u} -related LVM peaks in SI-29 for the range $T = 4 - 60 \text{ K}$. The inset in (a) shows the energy diagrams for the ^{29}Si - ^{16}O - ^{29}Si as discussed in the main text.

HgCdTe detector. A typical resolution was 0.03 cm^{-1} , and the signal-to-noise ratio was improved by co-adding 200 spectra.

III. RESULTS AND DISCUSSION

A. Assignment of modes to experimentally observed oxygen absorption lines

Previous studies have revealed that the interstitial oxygen has three major vibrational modes: A_{2u} , A_{1g} , and two-dimensional low-energy anharmonic excitation (2D LEAE, which has been also known as the low-frequency mode or 29-cm^{-1} mode).¹⁵ In most cases, experimentally obtained data have been analyzed using a model composed of the vibrating oxygen and its two nearest-neighbor Si atoms (Si-O-Si units) embedded in a homogeneous background of Si with the average masses determined by the isotopic abundance of ^{nat}Si (Refs. 10, 15, 20, and 21); i.e., the isotope shifts of the LVM frequencies have been calculated successfully for a variety of units such as ^{29}Si - ^{16}O - ^{29}Si , ^{29}Si - ^{18}O - ^{29}Si , ^{28}Si - ^{16}O - ^{29}Si , ^{29}Si - ^{16}O - ^{30}Si , etc. Figure 2(a) shows the A_{2u} -related absorption spectrum of the SI-29 sample obtained at 4 K. The inset shows an energy diagram of the A_{2u} -related excitations based on the notation $|k,l,N,M\rangle$,

TABLE II. Calculated and experimentally observed excitation frequencies of the $|0,0,0,0\rangle\text{-}|0,0,1,0\rangle$ transition.

| Configuration | Calculation [cm^{-1}] | Experiment [cm^{-1}] |
|---|----------------------------------|---------------------------------|
| $^{28}\text{Si}\text{-}^{16}\text{O}\text{-}^{28}\text{Si}$ | 1136.5 | 1136.5 |
| $^{28}\text{Si}\text{-}^{16}\text{O}\text{-}^{29}\text{Si}$ | 1134.1 | 1134.4 |
| $^{28}\text{Si}\text{-}^{16}\text{O}\text{-}^{30}\text{Si}$ | 1131.9 | 1132.0 |
| $^{29}\text{Si}\text{-}^{16}\text{O}\text{-}^{29}\text{Si}$ | 1131.7 | 1132.5 |
| $^{29}\text{Si}\text{-}^{16}\text{O}\text{-}^{30}\text{Si}$ | 1129.4 | 1130.8 |
| $^{30}\text{Si}\text{-}^{16}\text{O}\text{-}^{30}\text{Si}$ | 1127.0 | 1129.1 |
| $^{28}\text{Si}\text{-}^{18}\text{O}\text{-}^{28}\text{Si}$ | 1087.1 | 1084.4 |
| $^{29}\text{Si}\text{-}^{18}\text{O}\text{-}^{29}\text{Si}$ | 1079.8 | 1081.0 |

which has been employed in Refs. 15, 20, and 21. Here M , N , l , and k are the principal quantum number of the A_{1g} mode, principal quantum number of the A_{2u} mode, the angular momentum of the oxygen around the $\langle 111 \rangle$ axis, and an additional quantum number distinguishing the states of the same M , N , and l , respectively. Values of the energy separation shown in the inset are calculated for the $^{29}\text{Si}\text{-}^{16}\text{O}\text{-}^{29}\text{Si}$ configuration based on a harmonic model of a linear chain composed of one linear $^{29}\text{Si}\text{-}^{16}\text{O}\text{-}^{29}\text{Si}$ molecule surrounded by 196 Si atoms having an average mass of 28.966, which is in accordance with the isotopic composition of SI-29. The periodic boundary condition is imposed to eliminate the dangling bonds. The bonding constant connecting two Si atoms is $k_{\text{Si-Si}} = M_{\text{Si}}\omega^2/4 = 113.3 \text{ N/m}$, where M_{Si} is the average mass of Si atoms and $\omega = 524.6 \text{ cm}^{-1}$ is the TO phonon energy at the Γ point determined by the Raman spectroscopy of isotopically pure silicon crystals.⁴ The bonding constant between Si and oxygen, $k_{\text{Si-O}} = 479.18 \text{ N/m}$, is determined from the frequency of the A_{2u} mode of $^{28}\text{Si}\text{-}^{16}\text{O}\text{-}^{28}\text{Si}$ calculated by Yamada-Kaneta *et al.* (1151.5 cm^{-1}).¹⁵ We assume the same spring constants $k_{\text{Si-Si}}$ and $k_{\text{Si-O}}$ for any pairs of Si and O isotopes. A strong line at 1132.5 cm^{-1} observed experimentally in the main frame of Fig. 2(a) is due to the A_{2u} excitation from the $|0,0,0,0\rangle$ to $|0,0,1,0\rangle$ states of the $^{29}\text{Si}\text{-}^{16}\text{O}\text{-}^{29}\text{Si}$ configuration, which agrees very well with the estimation of the harmonic model shown in the inset. Figure 2(a) also shows several other LVM lines. The line at 1081.0 cm^{-1} is due to $|0,0,0,0\rangle\text{-}|0,0,1,0\rangle$ of $^{29}\text{Si}\text{-}^{18}\text{O}\text{-}^{29}\text{Si}$, 1201.4 cm^{-1} is $|0,0,0,0\rangle\text{-}|0,\pm 1,1,0\rangle$ of $^{29}\text{Si}\text{-}^{16}\text{O}\text{-}^{29}\text{Si}$, 1100.6 cm^{-1} is most likely carbon-oxygen complexes previously reported at 1103.9 cm^{-1} in $^{\text{nat}}\text{Si}$ (Ref. 22), and 1047.2 cm^{-1} may be related to the oxygen-impurity complexes discussed by Chappell *et al.*²³ The absorption line measured at 1207.7 cm^{-1} is probably irrelevant to oxygen LVM's since its amplitude does not follow the characteristic temperature dependence as shown in Fig. 2(b). In addition, LVM lines due to the $A_{2u} + A_{1g}$ combined mode of $^{29}\text{Si}\text{-}^{16}\text{O}\text{-}^{29}\text{Si}$ were observed at 1734.5 cm^{-1} ($|0,0,0,0\rangle\text{-}|0,0,1,1\rangle$) and 1727.6 cm^{-1} ($|0,\pm 1,0,0\rangle\text{-}|0,\pm 1,1,1\rangle$). A series of oxygen LVM peaks was also obtained with SI-28 and SI-30 samples, and the resulting first-order comparison of the peak position of $|0,0,0,0\rangle\text{-}|0,0,1,0\rangle$ determined from the experiments and calculation is shown in Table II. This table has been prepared only to show that our assignment of the specific mode to a corresponding peak observed experimentally is correct, though the exact

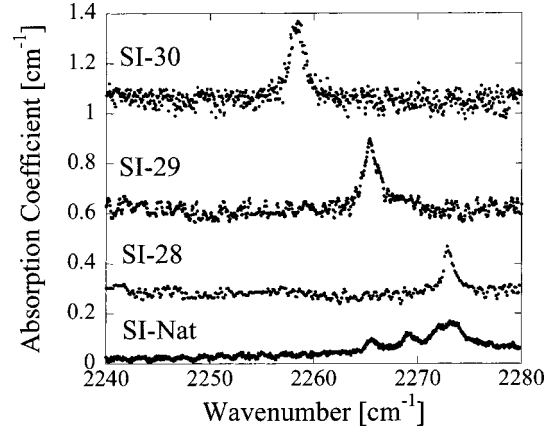


FIG. 3. Absorption peaks due to transitions from the ground to “ $A_{2u} + A_{2u}$ ” states for SI-28, SI-29, SI-30, and SI-nat samples.

peak position, for example, of $^{28}\text{Si}\text{-}^{16}\text{O}\text{-}^{29}\text{Si}$ shifts by 0.07 cm^{-1} between SI-29 and SI-nat samples as we will discuss later. Figure 2(b) shows the temperature dependence of the 1132.5 cm^{-1} excitation. As the temperature is raised, the low-frequency states such as 2D LEAE are excited. Therefore, the absorption intensities of the peaks at 1118.3 cm^{-1} ($|0,\pm 2,0,0\rangle\text{-}|0,\pm 2,1,0\rangle$ of $^{29}\text{Si}\text{-}^{16}\text{O}\text{-}^{29}\text{Si}$), 1124.5 cm^{-1} ($|0,\pm 1,0,0\rangle\text{-}|0,\pm 1,1,0\rangle$ of $^{29}\text{Si}\text{-}^{16}\text{O}\text{-}^{29}\text{Si}$), and 1126.40 cm^{-1} ($|0,\pm 1,0,0\rangle\text{-}|0,\pm 1,1,0\rangle$ of $^{28}\text{Si}\text{-}^{16}\text{O}\text{-}^{29}\text{Si}$) grow with increasing temperatures. Weak absorption lines at 1130.8 and 1134.4 cm^{-1} are $|0,0,0,0\rangle\text{-}|0,0,1,0\rangle$ of $^{29}\text{Si}\text{-}^{16}\text{O}\text{-}^{30}\text{Si}$ and $^{28}\text{Si}\text{-}^{16}\text{O}\text{-}^{29}\text{Si}$, respectively, for which the residual ^{28}Si (2.17%) and ^{30}Si (0.73%) isotopes in the SI-29 sample are responsible.

Figure 3 shows a series of LVM peaks centered around 2260 cm^{-1} not reported in the past. The LVM peaks at 2273.0 , 2265.7 , and 2258.4 cm^{-1} are obtained with SI-28, SI-29, and SI-30, respectively. Three broadened peaks with SI-nat at about 2273 , 2269.3 , and 2265.5 cm^{-1} are due to $^{28}\text{Si}\text{-}^{16}\text{O}\text{-}^{28}\text{Si}$, $^{28}\text{Si}\text{-}^{16}\text{O}\text{-}^{29}\text{Si}$, and $^{28}\text{Si}\text{-}^{16}\text{O}\text{-}^{30}\text{Si}$ configurations, respectively. These series of lines around 2260 cm^{-1} are most likely due to the $A_{2u} + A_{2u}$ combination since the values of isotope shifts are just twice as large as those due to the single A_{2u} mode. The isotope shift would be much larger if the 2260-cm^{-1} series is associated with the A_{1g} mode. These lines are observed clearly thanks to the small degree of mass disorder in our isotopically enriched samples. Figure 4 shows the temperature dependence of the “ $A_{2u} + A_{2u}$ ” combined mode in SI-30. The peak at 2241.9 cm^{-1} grows with increasing temperature. The value difference of 16.5 cm^{-1} ($=2258.4 - 2241.9 \text{ cm}^{-1}$) is just twice as large as the value difference of 8.0 cm^{-1} between the transition of $|0,0,0,0\rangle\text{-}|0,0,1,0\rangle$ (1129.1 cm^{-1}) and that of $|0,\pm 1,0,0\rangle\text{-}|0,\pm 1,1,0\rangle$ (1121.1 cm^{-1}). Then, from the experimentally obtained data, the peak measured at 2258.4 cm^{-1} must be due to the combined transition of $|0,0,0,0\rangle\text{-}|0,0,1,0\rangle$ and $|0,0,0,0\rangle\text{-}|0,0,1,0\rangle$ and the peak measured at 2241.9 cm^{-1} due to the combined transition of $|0,\pm 1,0,0\rangle\text{-}|0,\pm 1,1,0\rangle$ and $|0,\pm 1,0,0\rangle\text{-}|0,\pm 1,1,0\rangle$ in SI-30. However, we do not understand the reason why only such transitions were obtained since they are not allowed by the selection rule reported in Ref. 21. The LVM

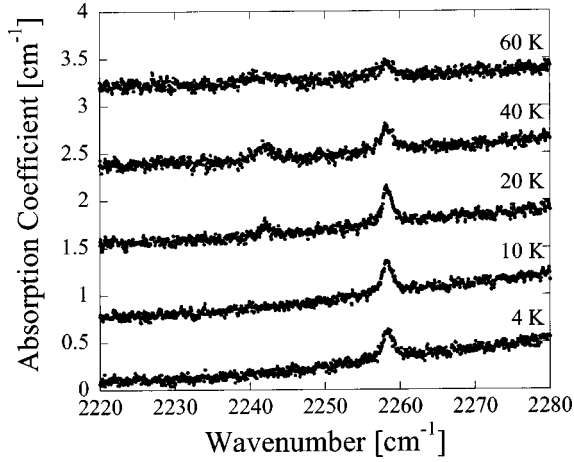


FIG. 4. Temperature dependence of the “ $A_{2u}+A_{2u}$ ” excited states for the SI-30 sample.

peaks observed in the present study (italic font) with those observed previously are summarized in Table III.

B. Host Si isotope effect on the oxygen LVM energy

We shall now discuss a very small peak position shift of $\sim 0.07 \text{ cm}^{-1}$ for the A_{2u} mode (the transition from $|0,0,0,0\rangle$ to $|0,0,1,0\rangle$) of the $^{28}\text{Si}-^{16}\text{O}-^{29}\text{Si}$ configuration observed between SI-nat and SI-29 samples as shown in Fig. 5. To first order one expects the LVM frequencies of the ^{16}O sand-

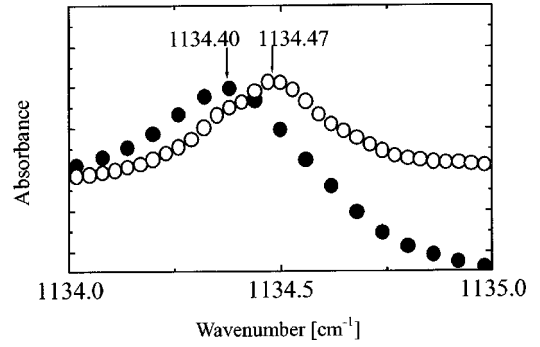


FIG. 5. LVM absorption peaks due to transitions from the ground to A_{2u} excited states of $^{28}\text{Si}-^{16}\text{O}-^{29}\text{Si}$ in the SI-29 (●) and SI-nat (○) samples measured at $T=4 \text{ K}$. The difference of frequencies between the two peaks is about 0.07 cm^{-1} .

wiched by ^{28}Si and ^{29}Si isotopes in SI-nat and SI-29 to be the same because the masses of the first neighbors predominantly determine the energy of the oxygen vibration. However, the peak position shifts as shown in Fig. 5 possibly due to two independent effects. One is the effect of the change in masses of the second and beyond nearest-neighbor silicon atoms to the vibrating oxygen. Those in SI-29 are mostly ^{29}Si , while those in SI-nat are mostly ^{28}Si isotopes. Calculations based on the linear chain model described above predict a shift of approximately 0.02 cm^{-1} . Figure 6 shows the amplitude of the displacement of each atom in our linear-chain calculation. For the case of the A_{2u} mode, the second-

TABLE III. LVM peaks previously reported in the past (Ref. 28) and reported in this study (bold italic printed values).

| $ k,l,N,M\rangle$ | Isotopic configuration of Si-O-Si (cm^{-1}) | | | | | | | |
|---|--|----------------------|----------|----------------------|----------------------|----------------------|----------|--------------------|
| | 28-16-28 | 28-16-29 | 28-16-30 | 29-16-29 | 29-16-30 | 30-16-30 | 28-18-28 | 29-18-29 |
| $ 0,0,0,0\rangle \rightarrow 0,\pm 1,0,0\rangle$ | 29.25 | | | | | | 27.2 | |
| $ 0,\pm 10,0\rangle \rightarrow 0,\pm 2,0,0\rangle$ | 37.7 | | | | | | 35.3 | |
| $ 0,\pm 1,0,0\rangle \rightarrow 1,0,0,0\rangle$ | 48.6 | | | | | | | |
| $ 0,\pm 2,0,0\rangle \rightarrow 0,\pm 3,0,0\rangle$ | 43.3 | | | | | | | |
| $ 1,0,0,0\rangle \rightarrow 0,\pm 1,0,0\rangle$ | 517 | | | | | | 517 | |
| $ 0,\pm 1,0,0\rangle \rightarrow 1,0,0,1\rangle$ | 668 | | | | | | | |
| $ 0,\pm 2,0,0\rangle \rightarrow 0,\pm 3,0,1\rangle$ | 664 | | | | | | | |
| $ 0,\pm 1,0,0\rangle \rightarrow 0,\pm 2,0,1\rangle$ | 657.4 | | | | | | | |
| $ 0,0,0,0\rangle \rightarrow 0,\pm 1,0,1\rangle$ | 648.2 | | | | | | | |
| $ 0,\pm 1,0,0\rangle \rightarrow 0,0,0,1\rangle$ | 588.4 | | | | | | | |
| $ 0,\pm 2,0,0\rangle \rightarrow 0,\pm 1,0,1\rangle$ | 580.2 | | | | | | | |
| $ 1,0,0,0\rangle \rightarrow 0,\pm 1,0,1\rangle$ | 570 | | | | | | | |
| $ 0,0,0,0\rangle \rightarrow 0,0,1,0\rangle$ | 1136.4 | 1134.4 | 1132.6 | <i>1132.5</i> | <i>1130.8</i> | <i>1129.1</i> | 1084.4 | <i>1081</i> |
| $ 0,\pm 1,0,0\rangle \rightarrow 0,\pm 1,1,0\rangle$ | 1128.2 | <i>1126.4</i> | | <i>1124.5</i> | | <i>1121.1</i> | 1076.7 | |
| $ 0,\pm 2,0,0\rangle \rightarrow 0,\pm 2,1,0\rangle$ | 1121.9 | | | <i>1118.3</i> | | <i>1114.7</i> | | |
| $ 0,0,0,0\rangle \rightarrow 1,0,1,0\rangle$ | 1205.7 | | | <i>1201.4</i> | | <i>1197.1</i> | | |
| $ 0,\pm 1,0,0\rangle \rightarrow 1,\pm 1,1,0\rangle$ | 1216.4 | | | | | | | |
| $ 0,0,0,0\rangle \rightarrow 0,0,1,1\rangle$ | 1748.6 | | | <i>1734.5</i> | | <i>1721.5</i> | 1150.8 | |
| $ 0,\pm 1,0,0\rangle \rightarrow 0,\pm 1,1,1\rangle$ | 1740.9 | | | <i>1727.6</i> | | <i>1714.2</i> | | |
| $ 0,\pm 2,0,0\rangle \rightarrow 0,\pm 2,1,1\rangle$ | 1734.1 | | | | | | | |
| $ 0,0,0,0\rangle \rightarrow 1,0,1,1\rangle$ | 1819.5 | | | | | | | |
| $ 0,\pm 1,0,0\rangle \rightarrow 1,\pm 1,1,1\rangle$ | 1831.3 | | | | | | | |

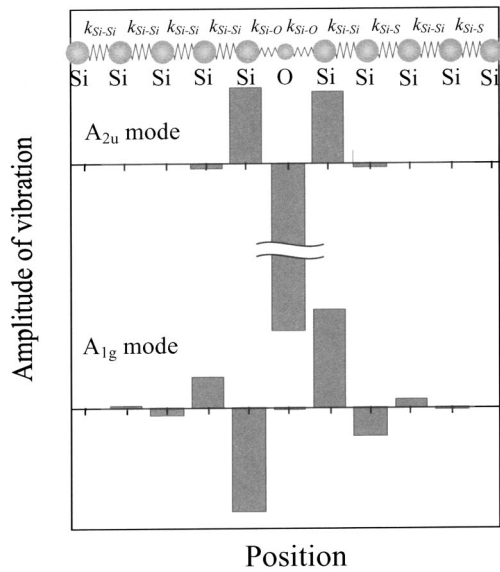


FIG. 6. Amplitudes of displacements for A_{2u} and A_{1g} modes of oxygen LVM's in silicon. A linear chain of one oxygen atom sandwiched by 198 Si atoms is employed as discussed in the text. The figure shows the displacements of only one oxygen atom and ten neighboring Si atoms.

nearest-neighbor Si atoms are clearly displaced: i.e., isotope substitution of the second neighbors should shift the LVM frequency. Although a much larger effect of the second and beyond nearest neighbors is expected for the A_{1g} mode as seen in Fig. 6, we could not observe A_{1g} -related absorption lines experimentally due to the insufficient thickness (<1 mm) of our sample. We suggest that the origin of large isotope shifts of the A_{1g} mode and the $A_{1g}+A_{2u}$ combined mode discussed in Refs. 14 and 21 may be due to the second and beyond nearest neighbors. In order to observe the effect of the second and beyond nearest neighbors on impurity LVM's, one has to select carefully the mass of the localized impurity and host semiconductors. For example, a hydrogen atom is so much lighter than the host Si atoms that its vibration is strongly localized, and the second-nearest Si atoms are not displaced at all. On the other hand, when the masses of the impurity and host atoms are too close, localization of the impurity vibration does not occur. For the case of oxygen in Ge, the mass difference is very large, and the shift attributed to the effect of the second and beyond nearest neighbors is only of the order of 0.010 cm^{-1} (Ref. 24). To our knowledge, the LVM of O in Ge and B in GaP (Ref. 25) are the only other examples that show the possible effect of the second and beyond nearest neighbors. Another possible origin of the shift is the isotope effect on the host silicon lattice constant. The fractional change of the lattice constant $\Delta a/a = -3.0 \times 10^{-5}$ has been reported for Si when passing from ^{28}Si to ^{29}Si at 30 K.²⁶ The LVM peak shift of $\Delta\omega = 0.065 \text{ cm}^{-1}$ is estimated from the relation $\Delta\omega = -3\gamma\Delta a/a\omega$, where $\omega = 1136.4 \text{ cm}^{-1}$ is the value of A_{2u} and $\gamma = -0.64$ is the Grüneisen parameter associated with the A_{2u} LVM reported in Ref. 27. The changes in the masses of the second and beyond nearest neighbors and in the host Si lattice constant both explain the observed shift of ~ 0.07

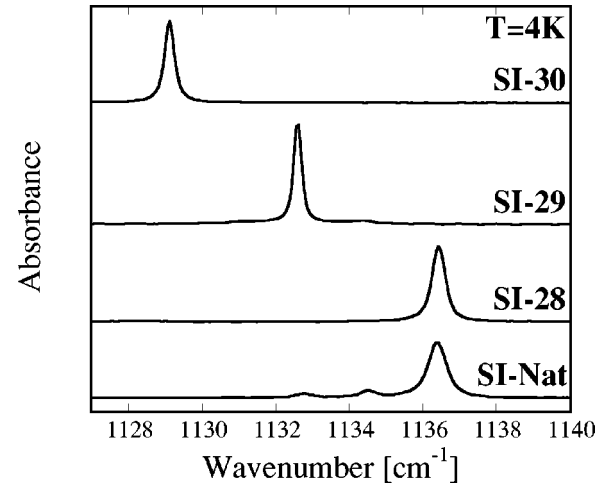


FIG. 7. Comparison of the width of the LVM lines of $|0,0,0,0\rangle$ - $|0,0,1,0\rangle$ transitions in SI-29, SI-28, SI-30, and SI-nat.

cm^{-1} for the A_{2u} mode of the ^{28}Si - ^{16}O - ^{29}Si configuration. Further investigations are necessary in order to separate these very interesting effects.

C. Isotope effects on the linewidth of oxygen LVM's

Up to here, we have successfully applied the harmonic approximation to explain the Si isotope shifts of the oxygen LVM frequencies. However, we shall now demonstrate the breakdown of the harmonic model especially when it comes to the linewidths of the oxygen LVM's. Figure 7 shows the absorption lines of the $|0,0,0,0\rangle$ - $|0,0,1,0\rangle$ excitation recorded with SI-nat, SI-28, SI-29, and SI-30 samples. The full widths at half maximum (FWHM) are 0.58 , 0.40 , 0.23 , and 0.30 cm^{-1} for SI-nat, SI-28, SI-29, and SI-30, respectively. Note that the amplitude of the peak at 1134.4 cm^{-1} in SI-29 we discussed in Fig. 5 is much smaller than that of the strongest peak at 1132.5 cm^{-1} : i.e., it is not evident in Fig. 7. First, we concentrate on comparing the results for SI-nat and SI-28. Since the average masses of the Si isotopes are very similar, we expect the phonon density of the states of these two samples to be the same. Therefore, the narrowing of the width in SI-28 with respect to that of SI-nat must not be due to the change in the phonon density of the states. The remaining possibility is the degree of the Si mass disorder, which is larger in SI-nat than in SI-28. In an attempt to reproduce theoretically the difference in the linewidths, we have calculated the full matrix elements of the oxygen LVM's for the three-dimensional structures shown in Fig. 1 with appropriate harmonic bond strengths k and K using the method employed in Ref. 15. However, we find a difference of only 0.02 cm^{-1} , which is factor of 10 smaller than the difference 0.18 cm^{-1} found by experiment. Therefore, we conclude that anharmonicity is playing an important role, together with differences in the degree of mass disorder. Moreover, further narrowing of the peaks in SI-29 and SI-30 is observed and it may be due to the combined effect of changes in the phonon density of the states (i.e., how easy it is for oxygen to relax via emission of lattice phonons) and isotope disorder. In the case of the A_{2u} mode (1136.4 cm^{-1}

in SI-nat), the LVM decays by the emission of at least three phonons since the maximum of the Si optical phonon frequency is 524.5 cm^{-1} . One possibility is the change in the so-called three-phonon density of states at the LVM frequencies: 1132.5 cm^{-1} for SI-29, 1129.1 cm^{-1} for SI-30, and 1136.4 cm^{-1} for SI-28 and SI-nat. $\text{FWHM}=0.23\text{ cm}^{-1}$ in SI-29 is 0.35 cm^{-1} smaller than $\text{FWHM}=0.58\text{ cm}^{-1}$ in SI-nat, in part due possibly to the smaller three-phonon density of the states at 1132.5 cm^{-1} in SI-29 than that at 1136.4 cm^{-1} in SI-nat, leading to a slower decay of oxygen vibrations, and in part due to the less Si mass disorder in the isotopically enriched SI-29 than in SI-nat, leading to less inhomogeneous broadening of the peak. Further investigations are needed clearly in order to fully understand the relation between the shift of oxygen LVM and the combined phonon density of states, both of which shift to lower wave numbers on passing from ^{28}Si to ^{30}Si . Our experimental results, however, suggest clearly that the enrichment of ^{29}Si isotopes towards 100% will sharpen the line beyond 0.23 cm^{-1} because of the surprisingly large contribution of the isotopic mass disorder to the width of the oxygen A_{2u} mode in silicon.

One note of concern is the effect of carbon on the linewidth of oxygen LVM's. The linewidth of oxygen LVM's in Si crystal is strongly sensitive to the carbon concentration since the carbon atom has a tendency to reside at the second nearest neighbor to the oxygen atom to form a carbon-oxygen complex.²² The LVM peaks of carbon-oxygen complexes were observed in SI-29 and SI-30, though the LVM of

isolated carbon was below the detection of limit of our system: i.e., the carbon concentration should be much less than 10^{17} cm^{-3} . The oxygen LVM peak may be changed if it were not for carbon in SI-29 and SI-30 samples.

IV. CONCLUSIONS

We have investigated the localized vibrational modes of oxygen in isotopically enriched ^{28}Si , ^{29}Si , and ^{30}Si single crystals. Isotope shifts of LVM frequencies from those in natural Si are clearly observed, and assignments of modes are given consistently to most of the peaks observed in this study. We have shown that the change in Si masses of the second and beyond nearest neighbors and the change in the lattice constants of the host Si crystals together play important roles in the determination of the oxygen LVM peak positions in silicon. The LVM linewidths of the A_{2u} mode in the enriched samples are found to be much narrower than those in natural Si. This observation suggests that the oxygen LVM linewidth is determined by both anharmonicity and inhomogeneous broadening due to isotopic disorder.

ACKNOWLEDGMENTS

We would like to thank Dr. H. Riemann and Dr. N. V. Abrosimov of Institut für Kristallzüchtung for the growth of the ^{28}Si and ^{29}Si single crystals. This work was supported in part by a Grant-in-Aid for Scientific Research in Priority Areas "Semiconductor Nanospintronics."

-
- ¹E. E. Haller, *J. Appl. Phys.* **77**, 2857 (1995).
²F. Widulle, T. Ruf, M. Konuma, I. Silier, M. Cardona, W. Kriegseis, and V. I. Ozhogin, *Solid State Commun.* **118**, 1 (2001).
³T. Ruf, R. W. Henn, M. Asen-Palmer, E. Gmelin, M. Cardona, H.-J. Pohl, G. G. Devyatych, and P. G. Sennikov, *Solid State Commun.* **115**, 243 (2000).
⁴D. Karaiskaj, M. L. W. Thewalt, T. Ruf, M. Cardona, H.-J. Pohl, G. G. Devyatych, P. G. Sennikov, and H. Riemann, *Phys. Rev. Lett.* **86**, 6010 (2001).
⁵D. Karaiskaj, M. L. W. Thewalt, T. Ruf, M. Cardona, and M. Konuma, *Phys. Rev. Lett.* **89**, 016401 (2002).
⁶Ken-ichiro Takyu, Kohei M. Itoh, Kunihiro Oka, Naoaki Saito, and Valerii I. Ozhogin, *Jpn. J. Appl. Phys., Part 2* **38**, L1493 (1999).
⁷A. D. Bulanov, G. G. Devyatych, A. V. Gusev, P. G. Sennikov, H.-J. Pohl, H. Riemann, H. Schilling, and P. Becker, *Cryst. Res. Technol.* **35**, 1023 (2000).
⁸Hyunjung Kim, R. Vogelgesang, A. K. Ramdas, S. Rodriguez, M. Grimsditch, and T. R. Anthony, *Phys. Rev. B* **57**, 15 315 (1998).
⁹R. C. Newman, *J. Phys.: Condens. Matter* **12**, R335 (2000).
¹⁰M. D. McCluskey, *J. Appl. Phys.* **87**, 3593 (2000).
¹¹D. R. Bosomworth, W. Hayes, A. R. Spray, and G. D. Watkins, *Proc. R. Soc. London, Ser. A* **317**, 133 (1969).
¹²H. J. Hrostowski and R. H. Kaiser, *Phys. Rev.* **107**, 966 (1957).
¹³H. J. Hrostowski and B. J. Alder, *J. Chem. Phys.* **33**, 980 (1960).
¹⁴B. Pajot, E. Artacho, C. A. Ammerlaan, and J.-M. Spaeth, *J. Phys.: Condens. Matter* **7**, 7077 (1995).
¹⁵Hiroshi Yamada-Kaneta, Chioko Kaneta, and Tsutomu Ogawa, *Phys. Rev. B* **42**, 9650 (1990).
¹⁶R. Jones, A. Umerski, and S. Öberb, *Phys. Rev. B* **45**, 11 321 (1992).
¹⁷B. Sun, A. Fraser, and G. Lüpke (private communication).
¹⁸A. J. Mayur, M. Dean Sciacca, M. K. Udo, A. K. Ramdas, K. Itoh, J. Wolk, and E. E. Haller, *Phys. Rev. B* **49**, 16 293 (1994).
¹⁹E. Artacho, F. Yndurain, B. Pajot, R. Ramirez, C. P. Herrero, L. I. Khirunen, K. M. Itoh, and E. E. Haller, *Phys. Rev. B* **56**, 3820 (1997).
²⁰Hiroshi Yamada-Kaneta, Chioko Kaneta, and Tsutomu Ogawa, *Phys. Rev. B* **47**, 9338 (1993).
²¹H. Yamada-Kaneta, *Phys. Rev. B* **58**, 7002 (1998).
²²G. Davies and R. C. Newman, in *Handbook on Semiconductors*, 2nd ed., edited by T. S. Moss (Elsevier, New York, 1994), Vol. 3, Chap. 21.
²³S. P. Chappell, M. Claybourn, R. C. Newman, and K. G. Barraclough, *Semicond. Sci. Technol.* **3**, 1047 (1988).
²⁴B. Pajot, E. Artacho, L. I. Khirunen, K. Itoh, and E. E. Haller, *Mater. Sci. Forum* **258–263**, 41 (1997).
²⁵A. Robbie, M. J. L. Sangster, E. G. Grosche, R. C. Newman, T. Pletl, P. Pavone, and D. Strauch, *Phys. Rev. B* **53**, 9863 (1996).
²⁶E. Sozontov, L. X. Cao, A. Kazimirov, V. Kohn, M. Konuma, M. Cardona, and J. Zegenhagen, *Phys. Rev. Lett.* **86**, 5329 (2001).
²⁷M. Pesola, J. von Boehm, T. Mattila, and R. M. Nieminen, *Phys. Rev. B* **60**, 11 449 (1999).
²⁸H. Yamada-Kaneta, *Physica B* **302–303**, 172 (2001).